

FIFTH INTERNATIONAL CONGRESS ON SOUND AND VIBRATION

DECEMBER 15-18, 1997  
ADELAIDE, SOUTH AUSTRALIA

## **LOW- AND MID-FREQUENCY FRF BASED MODELING OF ENGINE SUBFRAME AND CAR BODY INTERACTION FOR VIBRATORY AND ACOUSTICAL RESPONSE EVALUATION**

*K. Wyckaert\**, *G. Toniato\*\**, *K.Q. Xu\*\*\**

\* LMS International, Belgium; \*\* CRF, Italy; \*\*\* KULeuven, Belgium

### **ABSTRACT**

This paper describes the process of obtaining vibratory and acoustical response predictions within the car body, due to engine excitation. The approach that is followed, is to model the high modal density vibratory and acoustical behavior of the car body by a set of measured frequency response functions, while the engine carrying subframe is represented by a finite element model. The coupling interaction of the subframe with the car body is calculated based on FRF based substructuring techniques. The modeling process further includes experimentally derived engine excitation forces. Coupling predictions of subframe and car body are carried out and design changes evaluated.

### **1. INTRODUCTION**

Engine noise and vibration are very important components in the overall noise and vibration spectra in passenger car interiors. In this paper the structure-borne transmission mechanism of noise and vibration from the engine to the car interior is approached in a hybrid way. In order to model the transfer mechanisms from the engine over the subframe component into the car body, the car body component is represented by measurements, due to difficulties to model a fully trimmed car body up to higher frequencies, while the subframe can be represented by either measurements or by a validated FE model. In this paper, several modeling techniques are combined to investigate this engine-layout, subframe and car body interaction and the transfer of engine noise and vibration into the car. A schematic diagram of the process that was followed is shown in figure 1.

A finite element model of the subframe component was started from, in order to define a modal test on the prototype subframe component, which was tested in free-free conditions. The modal test was used to update a number of parameters in the finite element model in order to tune the resonance frequencies of the finite element model with the test model. At

the same time of the modal test, frequency response function measurements were performed on the free-free subframe component. Car body frequency response functions have been measured, including purely structural FRFs and vibro-acoustical FRFs. The coupled interaction between car body and subframe was addressed using FRF based substructuring, allowing to calculate the coupled frequency response functions between subframe and car body. Based on the given data set, this is done in a purely experimental approach or in a hybrid FE/experimental approach. Finally, based on the coupled model and the order-rpm representations of the engine running forces available at the engine mounting positions, a transfer path analysis is carried out. The objective is to identify the transfer mechanism and to propose possible structural modifications which will improve the structure borne engine order noise and vibration.

## 2. DESCRIPTION OF ENGINE-SUBFRAME-CAR BODY LAYOUT

Figure 2 schematically represents the subframe as it is attached to the car body in a number of bolted connections. The engine is supported in two points on the car body directly, while one support is on the subframe itself. In the process, the engine is considered as the source of vibration and noise and is not included in the test and analysis. The engine loading is represented by the engine induced forces, which enter at two places into the car body directly, while the forces as entering the mounting on the subframe are filtered by the subframe-car body interaction. The connections between the car body and the subframe consist of 4 bolts on the bottom of the car body and 2 near the front wheels, as indicated in figure 2. Acoustic pressure at the driver's head position and acceleration signals in 3 directions under the driver's seat are chosen as the response target signals inside the car-cavity.

### A Schematic View

#### Flow Diagram

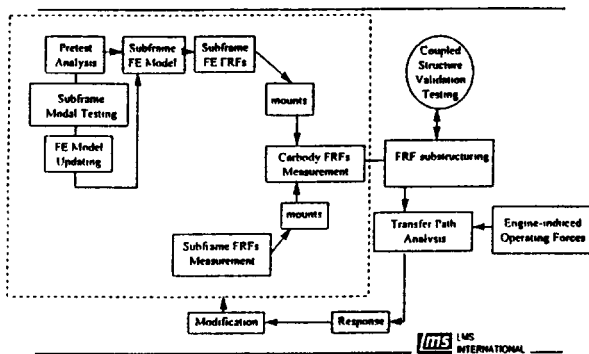


Figure 1. Flow chart of the process scheme

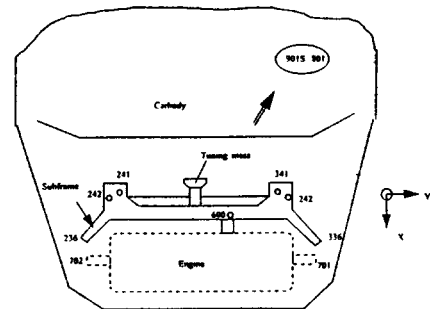


Figure 2. Schematical representation subframe-car body layout

### 3. FRF BASED SUBSTRUCTURING : THEORETICAL BACKGROUND

In order to allow calculation of the coupled effect of car body and subframe, the FRF based substructuring approach is used, where the components are represented by their frequency response functions in the connection points and in the target points of interest. This approach allows to represent the car body component by measured FRF data, which allows to extend the frequency range of interest beyond the modal frequency ranges. The component representation (in this case the subframe) can then come from calculation or from testing.

The theoretical formulation allows to calculate coupled frequency response functions between two subcomponents, as based on individual component representations (see also ref. [1-4]).

The kernel matrix equation to solve is the following :

$$\begin{bmatrix} [H_C]_{RR} & [H_C]_{RS} & [H_C]_{RT} \\ [H_C]_{SR} & [H_C]_{SS} & [H_C]_{ST} \\ [H_C]_{TR} & [H_C]_{TS} & [H_C]_{TT} \end{bmatrix} = \begin{bmatrix} [H_A]_{RR} & [H_A]_{RS} & 0 \\ [H_A]_{SR} & [H_A]_{SS} & 0 \\ 0 & 0 & [H_B]_{TT} \end{bmatrix} - \begin{bmatrix} [H_A]_{RS} \\ [H_A]_{SS} \\ -[H_B]_{TS} \end{bmatrix} \left\{ [H_A]_{SS} + [H_B]_{SS} + [K_s] \right\}^{-1} \begin{bmatrix} [H_A]_{RS} \\ [H_A]_{SS} \\ -[H_B]_{TS} \end{bmatrix}^T \quad (1)$$

in which, subscripts  $A, B$  refer to the two individual substructures in their free-free representation (to be coupled) and  $C$  to the coupled subsystem.  $R$  denotes the uncoupled DOFs of  $A$ ,  $S$  the coupling DOFs between  $A$  and  $B$ , and  $T$  the uncoupled DOFs of  $B$ , respectively;  $[K_s]$  is the stiffness matrix of possible flexible connectors, which in most cases is a diagonal matrix. In case of rigid coupling,  $[K_s]$  is infinite and its inverse becomes a zero matrix.

### 4. FRF SUBSTRUCTURING BASED ON PURELY EXPERIMENTAL FRFS

In the scheme of figure 1, two different approaches are followed. The substructuring of the subframe and the car body is based on a purely experimental approach, where for both subframe and car body measurements are taken, and on a hybrid FE/test approach, where the lower modal density subframe component is represented by a FE model and the car body by experiments. The car body is highly damped, which makes it very difficult to build a reliable car body modal test model or FE model. In this section we focus on the purely experimental substructuring.

#### 4.1. FRF Measurements

Hammer excitation was used to measure the frequency response functions of the free-free subframe (detached from the car body), the free-free car body (subframe was removed) and the coupled structure of car body and subframe. FRF measurements are done in between all connection points, as well as between the connection points and the input/output points. Input points include the engine attachment on the subframe; while output points include an acoustical response at the driver's ear, as well as a vibrational response on the car floor, under the driver's seat. For the subframe, two states were considered: one measurement

without the tuning mass, the other one with the tuning mass. For each case, a square FRF matrix of 21x21, representing input and output relations between all of these points of interest on the subframe, was measured. In contrast to the car body, the subframe shows a clear modal behavior. The tuning mass has a significant influence on the appearance of the FRFs. In general, the resonance peaks are left-shifted due to the added mass.

#### 4.2. Removal of accelerometer mass loading effects

Accelerometer mass loading was shown to be important on the subframe FRF measurements. Fig. 3 shows a comparison between a mass loaded subframe FRF (solid line) and one without mass loading (dotted line), measured using just one very small accelerometer (2 grams).

The conventional approach for mass loading correction is through free-interface mode synthesis based structural modification. To apply this method, one first needs to extract the modal parameters from the FRFs and then to modify these parameters by coupling with an imaginary “structure” which is represented by lumped negative masses. Finally, the modified parameters are used to re-construct for the FRFs which are free from mass loading. However, there are some disadvantages with this approach. They rely mainly in the fact that one usually takes into account a limited number of modes, which introduces approximations. The influence of higher modes out of the frequency band is also not accounted for. In view of the fact that for the FRF substructuring a full FRF matrix is measured anyhow, FRF substructuring can be used to remove the mass loading effects of the accelerometers, by coupling the subframe with an imaginary structure with negative lumped masses  $[-m_i]$  (diagonal matrix). Figure 3 shows the effect of the mass correction, next to the original FRFs.

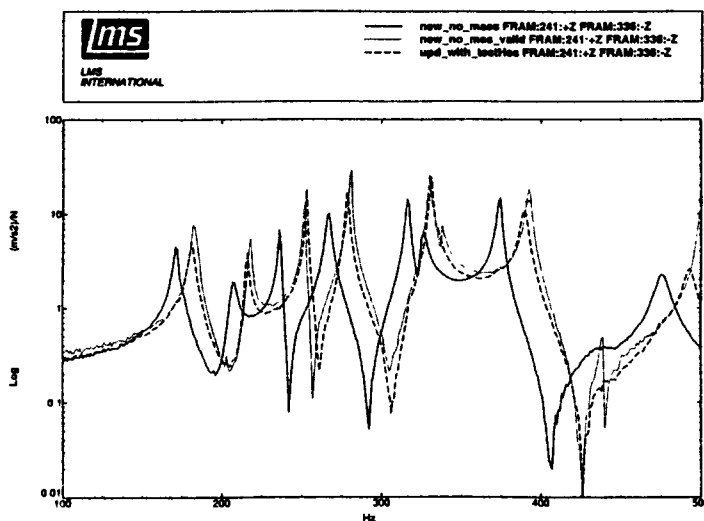


Figure 3. Accelerometer mass loading elimination: full line : measured FRF with mass loading, dotted line: measured FRF without mass loading, dashed line: corrected FRF for mass loading

### 4.3. Enhancing subframe FRFs via modal analysis and synthesis

Before starting the coupling analysis of the measured subframe FRFs and the car body FRFs, effort is put into minimizing the effects of the errors in the measured FRF data. For low modal density components, the anti-resonance areas in the free-free FRFs can suffer from noise. During the coupling procedure, this noise can be amplified significantly, which can additionally be influenced by bad conditioning of the matrix inversion in equation (1). For a high modal density well damped component like the car body, this is much less of a problem. Conditioning is usually much better, enhanced by the fact that during the measurements signal-to-noise ratios in all frequency areas are much better. For the low modal density component, the procedure involves enhancing the FRFs via modal analysis and synthesis. Particular care is taken to include rigid body effects and higher mode residual corrections in the FRF synthesis procedure, in order to account properly for truncation effects. Figure 4 shows a typical subframe FRF before (solid line) and after (dotted line) the enhancement. The modal smoothing effect on the FRF is evident especially in the anti-resonant regions where the signal-to-noise ratio is low.

The importance of this smoothing step for low modal density component FRFs where noise contaminates the data, is demonstrated through a simulated FRF substructuring analysis in which the subframe is coupled rigidly to the ground in its 4 car body connection points. The results, using the raw and the enhanced subframe FRFs respectively, are shown in figure 5. The general trend of the coupled FRFs with or without the enhancement are very close to each other. However, without the enhancement, the coupled FRF have many undesired ghost peaks which clearly do not reflect the modal properties of the grounded subframe. Using the enhanced FRFs, the results are also smoothed and exhibit a clear modal behavior which reflect the correct modal properties of the grounded subframe. The conditioning of the inversion process is not much affected by using enhanced FRFs or not. In the following, the enhanced subframe FRFs will be used in FBS computations.

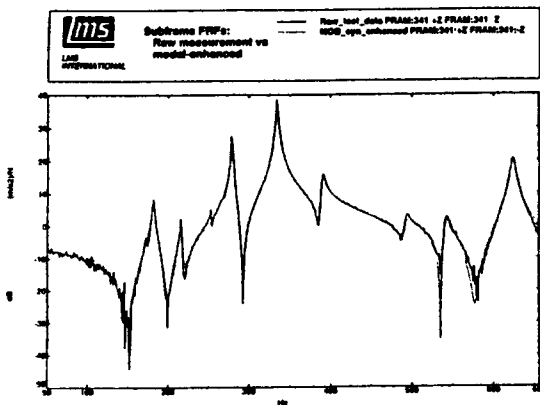


Figure 4. Raw free-free subframe FRFs (full line) as compared to enhanced FRFs via modal synthesis (dotted line)

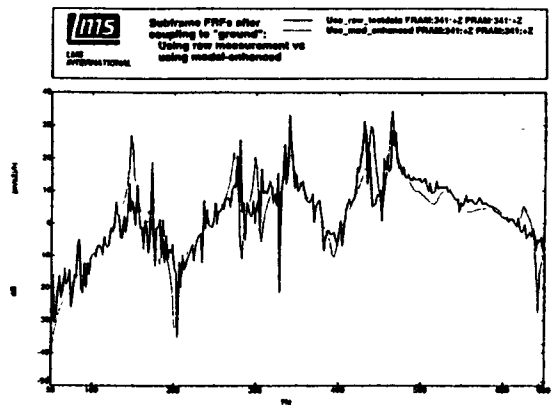


Figure 5. Coupled subframe FRFs (grounded conditions), based on raw measurement free-free subframe FRFs, as compared to based on enhanced subframe free-free FRFs

#### 4.4. FRF substructuring on measured car body FRFs and enhanced subframe FRFs

Figure 6 and 7 show the result of the modification of the tuning mass after the FRF substructuring on the vibro-acoustical and vibratory frequency response functions between the engine connection point on the subframe and the vibratory and acoustical response in the car body. The effect of the mass on these FRFs can be clearly seen.

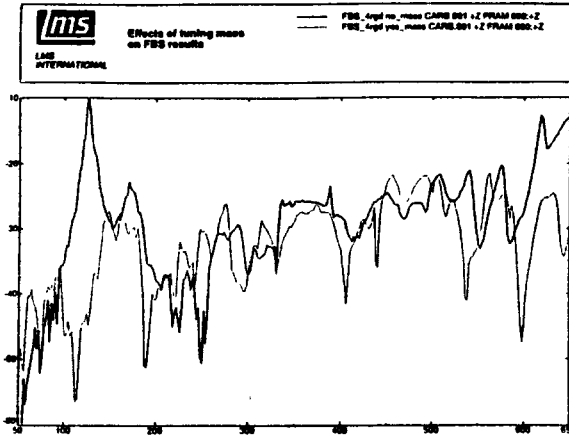


Figure 6. Predicted FRF between engine input point on subframe and a vibratory response point in car under driver's seat with (full line) and without tuning mass (dotted line)

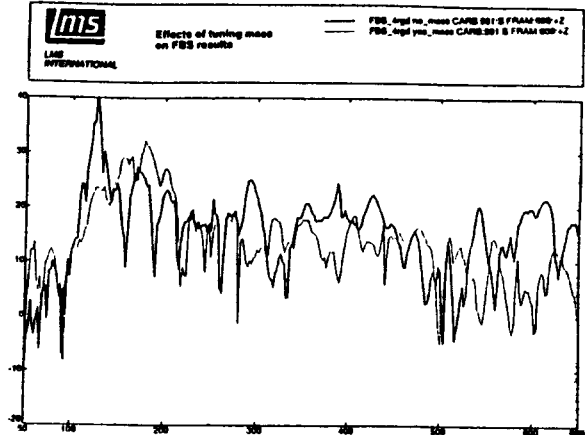


Figure 7. Predicted FRF between engine input point on subframe and a acoustical response point in car driver's ear with (full line) and without tuning mass (dotted line)

## 5. HYBRID FRF BASED SUBSTRUCTURING

In the scheme of figure 1, it is indicated that a hybrid approach is followed as well. This hybrid approach is mainly useful in earlier design stages, and allows FE models of more easy to model components to be combined with test data representing the more difficult to model car body component. In this case the FE model of the subframe was initially validated against component test data before the hybrid substructuring.

### 5.1. Pretest analysis on subframe FE model

The finite element model of the subframe (figure 8) has 5103 nodes and 5060 elements. A MSC/Nastran modal analysis was conducted. Using the LMS/Pretest software, the geometry of the FE model and the modes were used to define a wireframe model (figure 9) for modal testing. The calculated modes were used to determine the necessary measurement points and excitation points in order to avoid spatial aliasing by performing MAC calculations, and to excite all modes of interest.

The test consists of 11 response points and 2 input points. Accelerometer mass loading was avoided by attaching dummy masses at each of the measurement DOFs at the same time. FRFs were measured using independent burst random forces applied through two shakers. Modal analysis was performed.

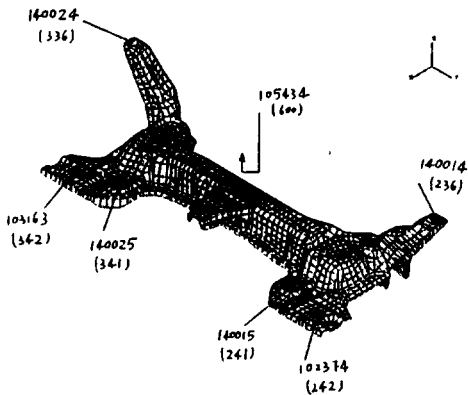


Figure 8. FE model of subframe

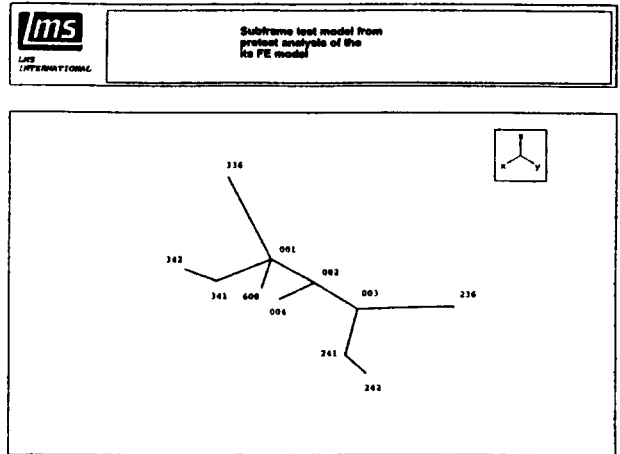


Figure 9. Test wireframe model of subframe

## 5.2. Correlation and Updating of Subframe FE Model

The masses of the accelerometers were added to the original FE model and a new NASTRAN modal analysis was performed. The results of the FE modal analysis and test modal analysis were read in LMS/Link. A correlation analysis was performed, based on MAC criteria. The results are documented in table 1.

The experimental modal analysis data were used to update the FE model. Possible model parameters to be updated are:

- plate thickness of components (12 parameters),
- the components are linked together by small beam elements, representing the welded connection. The cross section area, the two bending moments of inertia and the axial moment of inertia of these beams are the parameters of interest.

Based upon MSC/Nastran solution 200, for which LMS/Link acts as a pre- and a postprocessor, a sensitivity analysis of the modal frequencies upon these parameters was carried out. Figure 10 shows the result : the left axis represents the resonance frequencies, the right axis represents the parameter groups, the heights of the blocks represent the relative sensitivity of the parameters. Parameters like the moments of inertia of the beams are not sensitive, as well as a number of grouped shell thicknesses. This narrows down the parameter selection during the updating. The target of updating is the resonance frequency difference between the experimental model and the FE model for the lowest 5 modes.

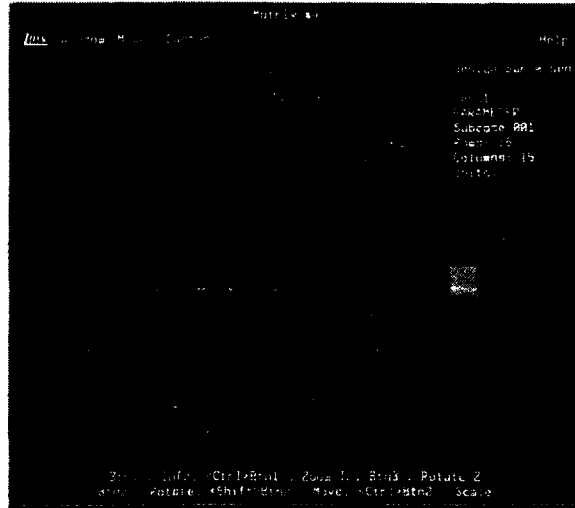


Figure 10. Frequency sensitivity analysis w.r.t. parameter sets in the FE model

The design optimization MSC/Nastran solution 200, as integrated within LMS/Link, was used to iteratively solve for the optimized parameters. The following table gives the frequency and MAC correlation of the resulting FE model with the modal test model. The first 4 resonance frequencies are in perfect agreement. The MAC values, however, decreased a little.

Test Frequency	FE Frequency	Freq. Diff. (%)	MAC	Test Frequency	FE Frequency	Freq. Diff. (%)	MAC
172.63	179.39	3.92	0.87	172.63	172.28	-0.20	0.84
204.95	228.55	11.51	0.71	204.95	204.73	-0.11	0.74
220.02	248.14	12.78	0.86	220.02	219.93	-0.04	0.85
260.50	310.99	19.38	0.86	260.50	260.37	-0.05	0.63
292.69	376.49	28.63	0.53	292.69	318.87	8.95	0.52
364.78	392.74	7.66	0.47	364.78	325.58	-10.75	0.45
464.76	435.26	-6.35	0.65	464.76	378.16	-18.63	0.66
432.53	435.26	0.63	0.63	432.53	378.16	-12.57	0.58
513.43	498.32	-2.94	0.70	513.43	439.42	-14.42	0.56
591.42	498.32	-15.74	0.40	591.42	439.42	-25.70	0.39
681.68	617.96	-9.35	0.66	681.68	561.00	-17.70	0.54
				749.55	598.70	-20.13	0.48

After the updating, the accelerometer masses were removed from the updated FE model, a new MSC/Nastran modal analysis was carried out and the resulting modes were used to synthesize for the FRFs among the DOFs of interest for coupling with the car body.

### 5.3. FRF Correction : Static and Dynamic Compensation

When synthesizing the frequency response functions from a limited number of FE modal vectors, it is important, certainly when using these FRFs for substructuring calculations, that residual effects of neglected higher order modes (modal truncation) are compensated for. This is done with the techniques of static and dynamic compensation (reference [5,6]).



For accelerance FRFs,

$$[H_s(\omega)] = [H_k(\omega)] + \frac{\omega^2}{\omega_1^2} ([H_c(\omega_1)] - [H_k(\omega_1)]) \quad (2)$$

$$[H_d(\omega)] = [H_s(\omega)] + \frac{\omega^4}{\omega_2^4} ([H_c(\omega_2)] - [H_s(\omega_2)]) \quad (3)$$

where  $[H_k(\omega_1)]$  is the sum of the contributions of the lower kept modes at the selected frequency points  $\omega_1$ , calculated by modal synthesis,  $[H_c(\omega_1)]$  and  $[H_d(\omega_2)]$  are, respectively, the non-truncated frequency response matrices at 2 selected frequency points  $\omega_1$  and  $\omega_2$ . In MSC/Nastran, the computation of the non-truncated frequency response matrix at a specific frequency point is supported through direct dynamic analysis. The computation work involved is equal to that of a static analysis.

In the subframe case, the two selected frequency points are  $f_1 = 20\text{Hz}$  and  $f_2 = 300\text{Hz}$ , and static and dynamic compensations are performed on top of the modal synthesis. In general, static compensation already improves the FRFs, especially in the lower frequency region. Dynamic compensation further improves the accuracy in the higher frequency region.

#### 5.4. Hybrid FRF Based Substructuring

The FRFs of the free-free subframe, synthesized and then dynamically compensated, from the updated FE modal analysis were used to couple with the experimental FRFs of the car body. Figure 11 shows the coupled vibratory transfer function between engine input point on the subframe and a vibratory response in the car for the case without (full line) and with tuning mass (dotted line). Figure 12 shows the vibro-acoustical FRF.

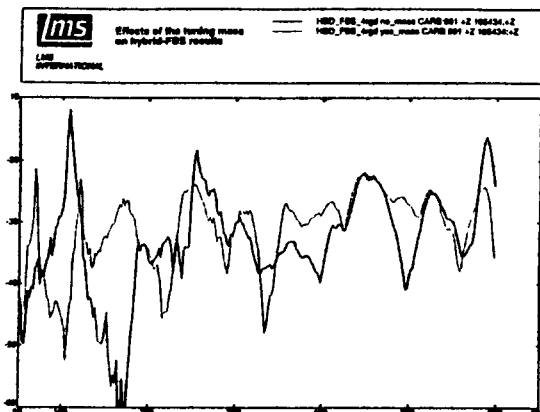


Figure 11. Predicted FRF between engine input point on subframe and a vibratory response point in car under driver's seat without (full line) and with tuning mass (dotted line) for hybrid case

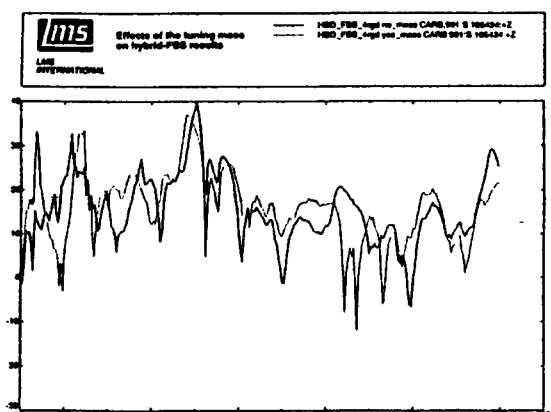


Figure 12. Predicted FRF between engine input point on subframe and a acoustical response point in car at driver's ear without (full line) and with tuning mass (dotted line) for hybrid situation

## 6. TRANSFER PATH ANALYSIS: FORCED RESPONSE ANALYSIS AND CONTRIBUTION ANALYSIS

Transfer path analysis is based on the relationship between the input  $\{F(\omega)\}$  and the output  $\{X(\omega)\}$  of a linear system described by its frequency response function representation  $[H(\omega)]$ , i.e.,

$$\{X(\omega)\} = [H(\omega)] \{F(\omega)\} \quad (4)$$

The input  $\{F(\omega)\}$  are the operating forces. The  $[H(\omega)]$  frequency response function matrix could be either directly measured from the coupled subframe-car body system or could be the result of the above FRF based substructuring analysis. The output  $\{X(\omega)\}$  are the responses which in this case include the acoustic pressure at the driver's ear and the acceleration response under the driver's seat.

In order to investigate the engine-induced vibro-acoustic response inside the car body, operating forces at the 3 engine mounts were indirectly identified from operating tests. The Z-direction second order acceleration response prediction in the target location in the car body is then given in figure 13, the acoustical second order response prediction is given in figure 14. The tuning mass is very effective for the acceleration response, but acoustically spoken does not contribute much. This is due to the relative interactions between all the 9 transfer paths, and the relative importance of the different paths with respect to each other.

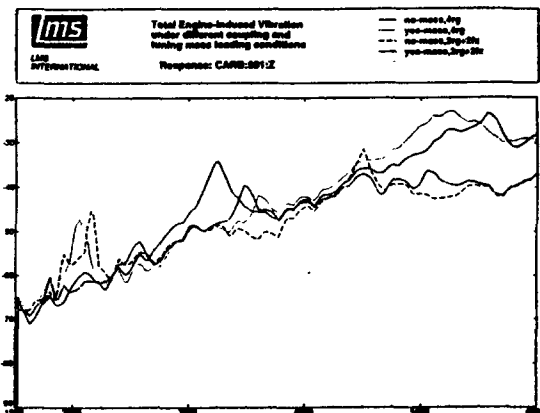


Figure 13. Comparison of second order prediction of interior car body vibratory operating response in different modification configurations (full line : with mass)

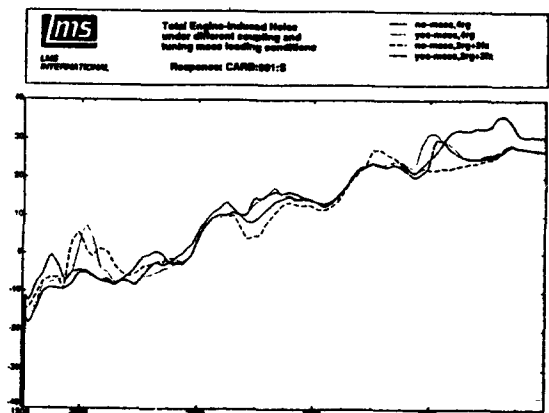


Figure 14. Comparison of second order prediction of interior car body operating acoustical response in different modification configurations (full line : with mass)

## **7. SUMMARY**

In this paper, several modeling techniques have been jointly applied to model the engine-layout, subframe and car body interaction and the transfer of engine order noise of a demonstrator car. Both a pure experimental FRF-based approach and a hybrid (experimental FRFs coupled with FE FRFs) approach have been taken. Some new techniques were developed in the paper, including static and dynamic compensations in synthesizing FRFs from the FE modal model, the enhancing technique (modal analysis and synthesis) of the measured FRFs and the removal of accelerometer mass loading effects from the measured FRFs. Compensations are necessary to minimize the truncation errors while synthesizing FRF from the FE modal model. Enhancement of test FRFs is effective in reducing the undesired noise effects on the coupled FRFs. A pretest analysis of the subframe FE model was carried out, providing a wireframe with only a few measurement points ready for use in the modal testing of the subframe. The identified modal data were used to update the FE model of the subframe. Finally, engine order noise and vibration were studied via transfer path analysis. Total responses are predicted and the relative importance of the transfer paths is compared.

## **8. ACKNOWLEDGEMENT**

Work described in this paper was carried out in the context of an EC sponsored BRITE-EURAM project BE 7796, for which the authors want to express their gratitude.

## **REFERENCES**

- [1] A. Klosterman, "On the Experimental Determination and Use of Modal Representations of Dynamic Characteristics", PhD Dissertation, Department of Mechanical and Industrial Engineering, University of Cincinnati, 1971
- [2] L. Bregant, D. Otte, P. Sas, "FRF Substructure Synthesis: Evaluation and Validation of Data Reduction Methods", Proceedings of 13<sup>th</sup> IMAC, Nashville, 1995
- [3] D. Otte, J. Leuridan, H. Grangier, R. Aquilina, "Coupling of Structures Using Measured FRFs by Means of SVD Based Data Reduction Techniques", Proceedings of 9<sup>th</sup> IMAC, Florida, 1990
- [4] K. Wyckaert, G. McAvoy, P. Mas, "Flexible Substructuring Coupling Based on Mixed Finite Element and Experimental Models: A Step Ahead of Transfer Path Analysis", Proceedings of the 14<sup>th</sup> IMAC, pp.633-640, Michigan, 1996
- [5] M.L.M. Duarte and D.J. Ewins, "Improved Experimental Component Mode Synthesis with Residual Compensation Based Purely on Experimental Results", Proceedings of the 14<sup>th</sup> IMAC, Michigan, February, 1996
- [6] K. Wyckaert, K.Q. Xu, P. Mas, "The Virtues of Static and Dynamic Compensations for FRF based Substructuring", Proceedings of 15<sup>th</sup> IMAC, 1997